TECHNICAL MEMORANDUMS

NATIONAL ADVISORY COMMITTEE FOR AERONAUTICS

No. 896



# THE DRAG OF AIRPLANE RADIATORS WITH SPECIAL REFERENCE TO AIR HEATING (COMPARISON OF THEORY AND EXPERIMENT)

By B. Göthert

Luftfahrtforschung, Vol. 15, No. 9, September 10, 1938
Verlag von R. Oldenbourg, München und Berlin



Washington
May 1939

NATIONAL ADVISORY COMMITTEE FOR AERONAUTICS

TECHNICAL MEMORANDUM NO. 896

# THE DRAG OF AIRPLANE RADIATORS WITH SPECIAL REFERENCE TO AIR HEATING (COMPARISON OF THEORY AND EXPERIMENT)*

By B. Göthert

## SUMMARY

1. The radiator core.- The ideal radiator core is the all-round heated single pipe cooled by a nonvortical air stream. From this optimum the ordinary radiator cores depart, principally for the following reasons:

a) Adverse cooling conditions due to the higher velocities in the radiator core, caused by the cross-sectional contraction as a result of the water ducts, cooling fins, etc.;

b) Separation losses on passing through the core at entry and exit as well as on the water tubes;

c) Temperature drop at the cooling fins which, for equal pressure loss, results in less heat removal.

By far the greater proportion of the additional losses, compared to those of the single pipe, is due to the sectional contraction which, however, can be counteracted in radiator installations by changing to greater radiator front areas with corresponding cooling-air throttling.

2. The unheated radiator in a duct - Flow through radiator.- The flow through unheated, ducted radiators in unseparated air flow can be computed from the pressure equation for undisturbed flow at the radiator exit.

---

*"Der Luftwiderstand von Flugzeugkühlern mit besonderer Berücksichtigung der Lufterwärmung (Vergleich von Theorie und Messung). Luftfahrtforschung, vol. 15, no. 9, September 10, 1938, pp. 427-444.

Since the discrepancy between the pressure at radiator exit and that of undisturbed flow is, in general, unpredictable on built-in radiators, the flow through built-in radiators should, preferably, be ascertained by a test.

Resistance of freely exposed radiator: In unseparated flow this can be computed sufficiently exact as the sum of the inside cooling resistance (i.e., of the drag of radiator core and of the pressure on diffuser and nozzle wall) and the frictional drag on the inside and outside surfaces of the ducts. Properly designed, the diffuser and nozzle losses are negligibly small.

Favorable diffuser design: In order to keep the frictional forces on the outside surfaces at a minimum, the diffuser mounted ahead of the radiator should, preferably, be no longer than consistent with the safe prevention of break-away of flow on the outside of the diffuser.

If the ratio of the diffuser orifice is smaller than the ratio of the nozzle orifice, very high additional separation losses usually occur within the diffuser. This means that at low flying speed, as in climbing, for instance, a case may occur where the radiator has to be adjusted at the outlet as well as at the inlet valve, in order to avoid flow-restricting separations within the diffuser.

3. The hot radiator in a duct.- The effect of heating on the drag and flow of the radiator is elaborated in formulas and diagrams, and checked on a number of measurements on freely exposed radiators.

If a ducted radiator is heated and the air flow is maintained even at all degrees of heating by corresponding valve adjustments, the radiator resistance changes in the following manner:

> By small pressure-drop coefficient of the cold radiator core and small axial-flow coefficient, the radiator resistance first decreases in increasing measure as the heating increases. But, beginning at a certain temperature, the drop in radiator resistance diminishes until at still greater heat the resistance of the heated radiator exceeds that of the cold radiator.

With great pressure-drop coefficient of the cold radi-

ator core and great axial-flow coefficient, the heating always induces a rise in radiator resistance.

4. The heated, built-in radiator - Additional drag of built-in radiators.- At small axial-flow coefficients, i.e., in the high-speed flight range, the built-in radiator discloses high additional resistances which, in general, amount to a multiple of the inside cooling drag and of the frictional drag on the radiator ducts. These added resistances are attributable to break-away of flow on the outside of the ducts and to the radiator wake, which alters the resistance of the body aft of the fuselage as regards frictional velocity, of the boundary layer, and of the pressure-field formation.

Since the radiator wake may disclose positive as well as negative pressure in relation to the free flow - depending upon the degree of radiator heating - the appraisal of these added resistances is contingent upon measurements with heated radiators.

Belly radiators and freely exposed radiators: Should the cited additional resistances be avoided when installing a radiator, the entire radiator resistance would be practically eliminated and, in special cases, even a lift produced.

The freely exposed radiator admittedly has very high friction losses on the large outside surfaces but, on the whole, they are less than half as high as the additional resistances on modern radiator systems.

Reduction of radiator resistance: The need at present of propitious radiator installation, with regard to low drag at high speed, is of paramount importance. Compared with it, the effect of radiator core efficiency and internal cooling drag are secondary.

## NOTATION

$Q$, heat removal in unit time.

$W_k = c_{wk} \frac{\rho}{2} v_1^2 F_K$, drag within the radiator core.

$W = c_w \frac{\rho}{2} v_o^2 F_K$ = cooling drag = internal drag of radiator + pressures on the diffuser and nozzle wall (no separation, no air friction on diffuser and nozzle walls, any radiator core).

$W_{min} = c_{w_{min}} \frac{\rho}{2} v_o^2 F_K$ = cooling drag + frictional forces on diffuser and nozzle walls for aerodynamically smooth surfaces (no break-away of flow, any radiator core).

$F_K$, frontal area of radiator.

$f$, free cross-sectional ratio of radiator core.

$p_o$, pressure of undisturbed free flow.

$\rho_o$, density of undisturbed free flow.

$T$, absolute temperature of free flow.

$v_o$, velocity of undisturbed free flow.

$v_1$, velocity directly before the built-in radiator core.

$\eta_{ac} = \frac{v_1}{v_o}$, coefficient of flow through radiator core.

ae?

$\eta_{ai} = \sqrt{\frac{1}{1+c_{wk}}}$, ideal permeability (i.e., percentage of open area) of core.

$\eta_{th} = \frac{\text{(air temperature at exit)-(air temperature at inlet)}}{\text{(radiator wall temperature)-(air temperature at inlet)}} =$

= thermodynamic quality of the radiator core.

$V_x$, notation for diffuser orifice ratio, i.e., entrance section = x percent of frontal area of radiator.

$H_x$, notation for nozzle orifice ratio, i.e., outlet section = x percent of frontal area of radiator.

## Indices

$T$, heated radiator.

$+$, referred to free cross-sectional area of radiator core.

w, referred to radiator wall.

0, far upstream from the radiator core.

1, directly in front of the radiator core.

2, directly behind the radiator core.

3, at exit from the radiator.

## INTRODUCTION

Since the radiator in an aerodynamically clean airplane shares an appreciable portion of the total drag of the airplane, and since this increases in significance as the engine horsepower and flying height are pushed up, it is of vital importance to know the limit to which the drag of radiators can be lowered. The knowledge of this minimum drag and the most prominent causes of the supplementary drag in actual radiators may afford some valuable information as to whether and to what points further studies in radiator-drag reduction might be profitably pursued.

To solve this problem, the most prominent reports - theoretical and experimental - on radiator research were surveyed, and supplemented and expanded where necessary.

### Survey of Past Radiator Research

On experimental reports concerning the aerodynamic and thermodynamic properties of radiator cores and radiator installations, a great number of investigations are available, of which the measurements on systematically ducted, freely exposed radiators of the Aachen Aerodynamic Institute (reference 4), and some measurements on differently ducted belly radiators in the big wind tunnel of the DVL are outstanding. In order to find from among this abundance of individual measurements the radiator most favorable for a certain flight condition in a certain type of airplane, various efficiency factors had been established - of which, for instance, one utilized the ratio of expendable radiator towing power to cooling horsepower for the appraisal of the radiator efficiency. The drawback of these experimentally obtained efficiency factors was that, while they afforded the partial resistances occurring on

the radiator in their entirety, they gave no clear separation of the different effects and hence no direct knowledge of the most important drag sources.

To obtain generally applicable rules for proper radiator installation, and at the same time some insight into the most important sources of loss, it was then attempted to divide the radiator drag mathematically into its components. Thus Weinig (DVL) computed the ideal drag for the unheated radiator, with the energy loss in the radiator core proper as sole source of loss, as premise. Kramer (DVL) supplemented this internal ideal drag with the friction drag on the inside and outside surfaces of the radiator ducts and an estimated diffuser loss, according to Fliegner, and arrived in this manner at conclusions about the quality of freely exposed and built-in radiators, as well as the correct throttling of the cooling air for high-speed aircraft. Schlupp's (DVL) and Barth's (Friedrichshafen) investigations (reference 5) aimed at inclusion of the other sources of loss, especially the additive drag due to separation of flow. Based upon measurements, they adduce methods according to which the estimation of the additional vortex loss is recommended for special types of installation.

Heating of the radiator frequently causes a drop in internal cooling drag as proved by Meredith (reference 6), with surprisingly simplified mathematical assumptions (for instance, the total heat removal by pressure at exit from the radiator core). This reduction in internal cooling drag may, in particular cases, even lead to an internal propulsion by flow through the radiator. Weise (reference 7) employed the fundamental relationship between heat transfer and wall friction to follow the physical change of the air on passage through the radiator in a pressure-velocity diagram, and so arrived at an exact solution of the effect of radiator heating. But since his numerical data available relate only to one specific case, supplementary calculations with regard to the heating effect on any other ducted radiators are necessary.

## Aim of the Present Study

Complementary to the past studies, the present report is intended as a systematic comparison of theoretical and experimental radiator drag, with the object of ascertaining the most important loss sources and their interaction in

different cases of installation, and to separate the radiator systems which are amenable to calculation, both as regards axial flow and drag. The sources of loss due to the diffuser are to be looked into closely as in many cases they can be of pre-eminent magnitude and their customary appraisal, according to Fliegner's formula, does not meet actual conditions. Besides, generally applicable equations and charts are developed for the rapid determination of the heating effect of radiators as regards flow and drag, and then checked by routine tests on hot radiators.

The equations which, on comparison of theory and test, proved in accord with actual conditions, are used for computing the minimum radiator drag for certain stipulated conditions of cooling, on the assumption of aerodynamically smooth surfaces and absolute avoidance of eddy separation. To exclude the weight effect in the determination of this minimum radiator drag, it was stipulated that the frontal area of the radiator should remain the characteristic quantity for the outside dimensions, and to so choose the radiator ducts that, for given outside cooling conditions - such as flying speed, cooling agent, air temperature, etc. - the radiator is capable of evacuating the given amount of heat. On these assumptions, the weight of the radiator is expected to change, even if different core design types are assumed, within such narrow limits, that the weight change can be ignored with respect to the total airplane weight.

## A. THE RADIATOR CORE

### I. HEAT OUTPUT AND PRESSURE DROP OF THE MOST PROMINENT RADIATOR CORES

Other than the weight, which according to the foregoing will be disregarded, the pressure drop and the heat removal characterize a certain radiator core. In conformity with the notation of the Aachen report (reference 3), the drag coefficient

$$c_{wk} = \frac{\Delta p}{\frac{\rho}{2} v_1^2} \quad (\text{IF } A_2 = A_1 \text{ ONLY})$$

serves as criterion for the pressure drop $\Delta p$ in the cold radiator core and the thermodynamic quality

$$\eta_{th} = \frac{T_2 - T_1}{T_w - T_1}$$

$$= \frac{\text{Air heating}}{\text{Temperature difference at entry in radiator}} = \frac{Q}{G\ c_p\ (T_w - T_1)}$$

as criterion for the heat removal $Q$.

$G$ is the weight of air passing through the radiator in unit time.

$c_p$, the specific heat of the air at constant pressure.

These coefficients $c_{wk}$ and $\eta_{th}$ are dependent upon the constant. For instance, by a change in flow velocity through the radiator, the pressure drop in first approximation would not change with the 2d power but, so far as it was created by friction losses, with the the 1.8th power of the axial flow; and the heat removal, rather than linearly, would approximately change with the 0.8th power of the axial flow velocity or of the air weight, $G$.

Figure 2 illustrates $c_{wk}$ and $\eta_{th}$ for cold radiator cores, as obtained from radiator tests in closed channel (reference 3). The pertinent radiators are appended in table I. The experimental curves are carried only as far as velocity $v_1 = 10$ m/s, since lower velocities are hardly permissible on radiators, and below this velocity the effect of laminar entrance length of the boundary layer on the drag and heat output, gains in importance.

## II. DEPARTURE OF ACTUAL RADIATOR CORE FROM THE IDEAL CORE

The plotted radiator data depart from the basic optimum values for equal air flow and equal heat removing surface for the following reasons:

a) Sectional contraction.- In accord with the Aachen

definition (reference 3), the pressure-drop coefficient, $c_{wk}$, is referred to the dynamic pressure directly before the radiator core, outside of the zone of influence of the radiator core. But, owing to the cross-sectional contraction, the velocity in the air passages of the radiator are higher than before the radiator. Then, as is known, the cooling at high air speeds is less favorable than at low speeds, because the drag increases in greater measure with rising air speed than the heat removal. For this reason, radiators with severely narrowed section are fundamentally inferior to those with little section contraction.

The pressure-drop coefficients $c_{wk}^{+} = f^2 c_{wk}$, reduced to mean dynamic pressure in the cooling passages, have been plotted against the thermodynamic quality $\eta_{th}$ in figure 3. It is seen that, for equal air heating, the pressure drop referred to tunnel speed, amounts to 30 to 50 percent in relation to the value referred to the speed before the radiator.

But this fundamental drawback of radiators with greatly narrowed cross section (reference 3) is usually immaterial in practical radiator installations, because in all modern cooling systems the flow is regulated by diffusers or nozzles.

b) Pressure drop.- Aside from the friction drag, which alone represents the equivalent for the heat dissipation, the generation of eddies also produces further drag, which in turn heightens the pressure drop without increasing the heat removal in equal measure. This eddy drag is produced, for instance, at entry and exit of the cooling air and, on water radiators, at flow around the water tubes.

c) Thermodynamic quality.- Even on radiators with indirect cooling surface, it is customary to refer the thermodynamic quality to the maximum wall temperature at entry in the radiator, despite the fact that the indirect cooling surfaces (fins) experience a temperature drop as a result of the cooling by the air flow. This drop in temperature lowers the heat removal in relation to that for identically high wall temperature. With unlimited good heat conductivity (heat transfer coefficient $\alpha \rightarrow \infty$) in fin material this temperature drop, and with it the drop in thermodynamic quality, would disappear.

These defects are fundamentally avoided on the all-

round, evenly heated tube, cooled by a nonvortical air flow (ideal radiator core).

The shifting of the ideal core curve in figures 2 and 3, indicates when the purely friction drag is supplemented by a constant drag proportion which does not promote heat removal. Leaving aside the shifting at low thermodynamic quality, figure 3 discloses that every single radiator core practically adjusts itself to these curves of equal supplementary drag, while the change-over to greater radiator depths, especially on water radiators, is followed by a shift to greater drag increases. The explanation for this is that the eddy drag on the presented radiator cores increases the pressure drop in greater measure than it improves the heat transfer, so that in its total effect it is to be considered detrimental.*

## III. INCREASE OF PRESSURE DROP IN RADIATOR CORE DUE TO HEATING

If the air, on flowing through the radiator block, becomes heated, it expands as a result of the temperature rise, and must therefore be accelerated to greater speed even in the cooling passages. On the other hand, the higher air speed in conjunction with the greater viscosity of the heated air, raises the friction drag on the walls of the cooling passages. The air acceleration and the increased friction drag in turn involve, for equal air flow, a greater pressure drop than on the unheated radiator block.

*Weise (reference 7) accounted for the deviation of the actual from the ideal radiator core with an empirical core constant $\Omega$. In the $\eta_{th} = f(c^{+}_{wk})$ chart, for instance, $\Omega$ denotes the factor with which the drag of the ideal tube must be multiplied in order to obtain, by equal air heating $\eta_{th}$, the drag coefficient $c^{+}_{wk}$ of the related radiator corps. According to figure 3, the assumption of a constant $\Omega$ value, independent of radiator depth and speed, approximately represents the curve variation of air-tube radiators, but on water-tube radiators every cooling system manifests marked discrepancies (cooling system 5, particularly). These discrepancies are attributable to the eddy drag on flowing around the individual water tubes.

1. Calculation of Pressure-Drop Increase

According to the law of momentum, the friction force $W^+_{rx}$ applied on the walls of the cooling tube must be equal to the momentum change of air flow between the related sections (fig. 4):

$$W^+_{rx} = \frac{G}{g}\left(v_1^+ - v_x^+\right) + \left(p_1^+ - p^+_{x_T}\right) F_k^+$$

$$= \int_0^{x/l} c^+_{wk_x} \frac{\rho x}{2} v_x^{+2} F_k^+ \, d\left(\frac{x}{l}\right)$$

Introducing then Blasius' (reference 8) local friction coefficient of pipes with $c^+_{wk_x} \sim \left(\frac{\nu_x}{v_x^+}\right)^{0.25}$ (on the assumption that this law retains its validity if in stream direction the density $\rho$, the viscosity $\nu$, and the speed $v$ are variable; the errors can only be quite small because it involves only the fourth root), while bearing in mind that the stream density $(\rho_x v_x^+)$ must be constant according to the law of continuity, a few transformations leave:

$$\frac{p^+_{x_T} - p_1^+}{\frac{\rho}{2} v_o^2} = - \eta^{+2}_{ae_T}\left[c^+_{wk} \int_0^{x/l} \left(\frac{v_x^+}{v_1^+}\right)^{0.75} \left(\frac{\nu_x}{\nu_1}\right)^{0.25} d\left(\frac{x}{l}\right) + 2\left(\frac{v_x}{v_1} - 1\right)\right]$$

The air viscosity $\nu$ increases, as is known, at constant pressure, about quadratically with the absolute temperature ratio (fig. 5), hence may be written in the form:

$$\frac{p^+_{x_T} - p_1^+}{\frac{\rho}{2} v_o^2} = - \eta^{+2}_{ae_T}\left[c^+_{wk} \int_0^{x/l} \left(\frac{v_x^+}{v_1^+}\right)^{0.75} \left(\frac{T_x}{T_1}\right)^{0.5} d\left(\frac{x}{l}\right) + 2\left(\frac{v_x}{v_1} - 1\right)\right]$$

The increased pressure drop due to the heating and hence the absolute pressure $p^+_{x_T}$ can, accordingly, be computed on every point of the tube, provided the temperature distribution and the correlated speed increase along the tube are known.

Disregarding the effect of the pressure change on the air density, as previously done in the calculation of the cold radiator, it simply follows that the velocities in the cooling channel change in the same ratio and air density in the inverse ratio of the absolute temperatures.*

---

*With inclusion of the density change due to pressure drop in the tubes, the gas equation stipulates that $v^+_x \sim T_x/p^+_{x_T}$. But, since we are primarily concerned with the drag discrepancy between hot and cold radiator, and the cold radiator in section B,I is computed for constant density, the calculation of the heated radiator must proceed on the basis of the excessive pressure drop in relation to pressure drop $\Delta p^+_x$ of the cold radiator for the density change instead of the total pressure drop $\Delta p^+_{x_T}$; i.e., $\frac{v^+_x}{v^+_1} = \frac{p^+_x}{p^+_{x_T}} \frac{T_x}{T_1}$. Posing, for the purpose of estimating the pressure-drop effect on the air density, the pressure drop of the heated radiator, in accord with equation (1), the omission of small terms (i.e., overestimation of pressure effect on air density), leaves:

$$\frac{p^+_{x_T}}{p^+_x} = 1 - \eta^2_{ae_T} \frac{\frac{\rho}{2} v_o^2}{p_o} \frac{\eta_{th} (T_w - T_1)}{T_1} \times \left[\frac{5}{8} c_{wk} \left(1 + \frac{1}{6} \eta_{th} + \frac{1}{12} \eta_{th}^2\right) + \frac{2}{f^2}\right]$$

and for the velocity ratio:

$$\frac{v^+_x}{v^+_1} = \frac{T_x}{T_1} \left\{1 + \eta^2_{ae_T} \frac{\frac{\rho}{2} v_o^2}{p_o} \frac{\eta_{th} (T_w - T_1)}{T_1} \times \left[\frac{5}{8} c_{wk} \left(1 + \frac{1}{6} \eta_{th} + \frac{1}{12} \eta_{th}^2\right) + \frac{2}{f^2}\right]\right\}$$

With $\eta_{ae}$ of the order of magnitude of 0.3 and $\frac{\rho}{2} \frac{v_o^2}{p_o}$ about = 0.10, it gives for high-temperature liquid cooling:

$$v^+_x/v^+_1 = \sim 1.003 \times T_x/T_1$$

(Continued on p. 13)

With this equation (3) becomes:

$$\frac{p^+_{x_T} - p^+_1}{\frac{\rho}{2} v_0^2} = - \eta^{+2}_{ae_T} \left[ c_{wk} \int_0^{x/l} \left(\frac{T_x}{T_1}\right)^{1.25} d\left(\frac{x}{l}\right) + 2\left(\frac{T_x}{T_1} - 1\right)\right]$$

This equation hides as yet the effect of heating in the absolute temperature ratio of the cooling air. Initial and terminal temperature of the cooling air are already given from the measured thermodynamic quality $\eta_{th}$ so that only the law for the temperature distribution within these limits need be found.

Now a special consideration proved* that the temperature distribution in a heated pipe cannot be essentially unlike that obtained from an assumption of constant material values ($\rho$, $\lambda$, a, etc.), so that the use of approximate law should involve no great error (reference 9, p. 57):

$$\frac{T_x}{T_1} = 1 + \frac{T_w - T_1}{T_1}\left[1 - (1 - \eta_{th})^{x/l}\right]$$

---

(Continuation of footnote from p. 12)
This example shows that the chosen equation $v^+_x/v^+_1 = T_x/T_1$ is practically correct.

*According to Merkel (reference 9), the coefficient of heat transfer $\alpha$ in pipes is:

$$\alpha \sim \lambda \left(\frac{v\,d}{a}\right)^{0.79}$$

($\lambda$ is the heat conduction of air; d, pipe diameter; a, temperature conductivity); i.e., the heat transfer coefficient $a_x$ at section x is to the heat transfer figure $\alpha_1$ at entry in the pipe:

$$\frac{\alpha_x}{\alpha_1} = \frac{\lambda_x}{\lambda_1}\left(\frac{v^+_x}{v^+_1}\frac{a_1}{a_x}\right)^{0.79} = \sim \frac{\lambda_x}{\lambda_1}\left(\frac{T_x}{T_1}\frac{a_1}{a_x}\right)^{0.79}$$

For instance, at an air inlet temperature of $T_1 = 230^\circ$ Abs., and an outlet temperature of $T_x = 350^\circ$ Abs., it affords $\alpha_{350}/\alpha_{230} = 1.065$; i.e., the rise in heat transfer figure toward the end of the pipe amounts to only 6.5 percent by this extreme temperature ratio. The temperature rise from $T_1$ to $T_2$ is very little shifted by this change in heat transfer figure; the maximum discrepancy with accurate allowance for the local heat transfer $\alpha_x$ was found to be less than 0.4 percent of the absolute inlet temperature, as confirmed by graphical integration.

Then integration and series development give the comparative increase in pressure drop in relation to the unheated radiator core in equal air flow as:

$$\frac{\Delta p_T^+ - \Delta p}{\Delta p} = \frac{c_{wk_T}^+ - c_{wk}^+}{c_{wk}^+}$$

$$= \eta_{th} \frac{T_w - T_1}{T_1} \left[ \frac{5}{8} \left( 1 + \frac{1}{6} \eta_{th} + \frac{1}{12} \eta_{th}^2 \right) + \frac{2}{f^2 c_{wk}} \right] \quad (1)$$

$\Delta p = \frac{\rho}{2} v_o^2 \eta_{ae}^{+2} c_{wk}^+$ = pressure drop of cold radiator,

$\Delta p_T^+ = \frac{\rho}{2} v_o^2 \eta_{ae}^{+2} c_{wk_T}^+$ = pressure drop of heated radiator (measured between beginning and end of tube).

In this equation the term $\left( 1 + \frac{1}{6} \eta_{th} + \frac{1}{12} \eta_{th}^2 \right)$ indicates the law, according to which the temperature of the cooling air rises from its original temperature $T_1$ to the prescribed terminal temperature $T_2$. The effect of this law on the increased pressure drop due to heat is seen to be unimportant.

The equation states that on radiator blocks with small drag coefficient $c_{wk}$, the necessary air acceleration as a result of warming governs the increase in pressure drop during heating (characterized by term $\frac{2}{f^2} c_{wk}$), but that on radiator blocks with high drag coefficient $c_{wk}$, the predominant effect is exerted by the greater wall friction due to the great air speed and viscosity (characterized by the term $\frac{5}{8} \left( 1 + \frac{1}{6} \eta_{th} + \frac{1}{12} \eta_{th}^2 \right)$).

## 2. Comparison of Theory and Measurement

As a check on the calculation of the pressure drop in a radiator core due to heating, several pressure-drop records for a flat-tube radiator (reference 3) from the Aachen Aerodynamic Institute were available (fig. 6). The pressure drop had been measured as pressure difference in the flow directly before and behind the actual radiator block,

hence still contained the difference between the pressure decrease due to flow acceleration at entry into the narrowed tubes and, on the other hand, to the pressure increase due to flow deceleration of the meanwhile heated air from the narrowed passages. In relation to the cold radiator block, the following dynamic pressure rise is therefore included in the measurement:

Dynamic pressure gain = (pressure loss at entry in tube) + (pressure gain at exit),

$$\frac{\Delta p_T - \Delta p_T^+}{\frac{\rho}{2} v_o^2} = \frac{\rho_T}{\rho_o} \left(\frac{T_2}{T_1}\right)^2 \eta_{ae_T}^{+2} (f^2 - 1) + \eta_{ac_T}^{+2} (1 - f^2)$$

Accordingly, the pressure loss in the tubes, in agreement with equation (1), must be supplemented by the following pressure gain:

$$\frac{\Delta p_T - \Delta p_T^+}{\Delta p} = \frac{-(1 - f^2)}{f^2} \frac{\eta_{th} (T_w - T_1)}{T_1} \frac{1}{c_{wk}} \qquad (2)$$

The increases in pressure drop, computed according to equations (1) and (2) for the Aachen experimental flat-tube radiator together with the test values, are plotted in figure 7. The theoretical values are a little lower than the measured values, although a mean line drawn through the test points yields the same rise as the computed curve. It is probable that on plotting the test data the base point, i.e., the pressure drop of the cold radiator, was determined about 2 percent too small, which a minor error in measurement would account for. On that assumption, the agreement is practically complete.

Here also was available a measurement of increased pressure drop due to heating, published by Parsons and Haper (reference 1), who investigated a round-tube radiator in the cold state and at a 61° C. temperature difference between water and air inlet temperature. For this case the calculation showed an increase in pressure drop in the core averaging 17.5 percent as against 16.5 percent in the diagram. The agreement therefore is quite good.

Herewith it is proved, at least for the temperature range measured, that the fundamental assumptions for the

heated radiator, namely, the proposed velocity increase as a result of the temperature rise and the temperature distribution in a heated tube, are accurately enough fulfilled for practical purposes.

## B. RADIATOR INSTALLATION AND DUCTS

### I. THE UNHEATED RADIATOR

For the sake of simplicity in the calculation of the unheated radiator, the compressibility of the air - i.e., the density change of air due to the variable pressure along a streamline - is disregarded. At the speeds of the present high-speed airplanes, the effect of this omission is as yet unimportant, as may be concluded from the small effect of the air density changes on other flow phenomena at equal speeds as, for instance, on the flow around airfoils.*

Flow phenomena are easiest to follow on a freely exposed, ducted radiator; i.e., a radiator towed to such distance from the airplane that the flow at the radiator may be considered as unaffected. In this specific case, all sources of loss arising from mutual interference of flow around the airplane and radiator - for instance, as regards boundary-layer formation - disappear. However, the results were so combined or extended that they can also be applied to any other radiator - as ventral radiators, for instance - provided that the same assumptions, such as aerodynamically smooth surfaces and nonseparating design, hold true for the radiator installation.

---

*The cooling air heats up in the diffuser as a result of the compression, which lowers the effective temperature difference between cooling air and radiator wall. On very fast airplanes, with small temperature differences between radiator wall and entering air, it is advisable to allow for this reduction in effective temperature difference, as, for instance, according to the approximate formulas in reference 6.

## 1. Flow through Unheated Radiator

a) Rate of flow.- Figure 9 depicts a ducted free-running radiator; the cooling air flows first through the diffuser 0 to 1, where the velocity of $v_0$ in the undisturbed flow is decreased to $v_1 = \eta_{ae} v_0$. After passing through the core proper (1 to 2) where at equal velocity the pressure drops by

$$\Delta p = c_{wk} \frac{\rho}{2} v_1^2 = c_{wk} \eta_{ae}^2 \frac{\rho}{2} v_0^2$$

the air is speeded up again in the nozzle (2 to 3).

Because of the displacement effect of the radiator, the air outside flowing around the radiator must travel faster than the corresponding velocity of the undisturbed flow. With increasing distance from the radiator inlet, this velocity increase gradually diminishes and disappears altogether at great distance behind the radiator. This disappearance of the velocity increase is usually so rapid, even with short radiator ducts, that by the time it reaches the exit of the radiator, the velocity of undisturbed flow practically exists again and consequently, also the pressure of undisturbed flow. (See flow measurements on cowling H 100, in fig. 12.)

Assuming the pressure of undisturbed flow $p_0$, at the end of the nozzle, a certain nozzle contraction $F_3/F_2$ and drag coefficient $c_{wk}$ of the built-in core, the proper expansion ratio $F_1/F_0$ of the interposed diffuser and the axial-flow velocity $v_1 = \eta_{ae} v_0$ can be computed. It is:

Pressure rise in diffuser - pressure loss in core
= pressure loss in nozzle

$$\frac{\rho}{2} v_0^2 (1 - \eta_{ae}^2) - c_{wk} \eta_{ae}^2 \frac{\rho}{2} v_0^2 = \eta_{ae}^2 \left(\frac{F_2^2}{F_3^2} - 1\right) \frac{\rho}{2} v_0^2$$

Hence

$$\eta_{ae}^2 = \frac{1}{c_{wk} + (F_2/F_3)^2}$$

or, using the ideal flow figure $\eta_{ai} = \sqrt{\frac{1}{1 + c_{wk}}}$

$$\eta_{ae}^2 = \frac{1}{\frac{1}{\eta_{ai}^2} + (F_2/F_3)^2 - 1} \tag{3a}$$

In similar manner we find for built-in radiators (for instance, for ventral radiators) where the pressure of free flow at the point of nozzle exit opening manifests a pressure difference $p_3 - p_o = \Delta p_a$ relative to the pressure of undisturbed free flow:

$$\eta_{ae}^2 = \frac{1 - \frac{\Delta p_a}{\frac{\rho}{2} v_o^2}}{\frac{1}{\eta_{ai}^2} + (F_2/F_3)^2 - 1} \tag{3b}$$

The problem of the diffuser then consists in decelerating the flow to $\eta_{ae}\, v_o$, so that with a fitting diffuser the orifice ratio $F_o/F_1 = \eta_{ae}$ must be chosen. Now, however, the problem of the diffuser can, to a substantial proportion, be taken over without loss by the free flow itself without outside guide surfaces, because the free flow itself dams up before a resistant body, and the streamlines are outwardly deflected (fig. 10) as a result of the higher pressure in the zone of low speeds.

Then the problem of the shortened diffuser merely consists of deflecting the outward pushing streamlines in the direction of the radiator tubes; its effect is the same as that of the airfoil, which deflects a certain volume of air per second by a certain angle from the original direction of flow (reference 7). So long as there is no separation of the stream, an airfoil produces always the same lift, independently of the wing chord if the entrained quantity and deflection are kept even. With decreasing wing chord, of course, the lift per unit area increases until the maximum lift coefficient is reached. Since on the diffuser - at equal air flow - the amount of air and the resultant angle of deflection are independent of the length of the remaining diffuser rest, the force effect on the diffuser wall itself is independent of the diffuser length. But, as on the airfoil, shortening the diffuser

length increases the diffuser force per unit surface which, corresponding to the maximum lift coefficient, cannot exceed a certain limit. On overly shortened diffusers the flow would have to be too sharply deflected, causing the stream to separate on the outside of the diffuser and create additional losses through burbling. On the other hand, on a diffuser with contraction ratio smaller than $\eta_{ae}$ (fig. 11), the streamlines bunched together at entry in the diffuser, are sharply deflected into the outwardly spreading direction, thus increasing the hazard usually existing in diffusers - separation of flow on the inside walls. The too-narrow diffusers are distinctly sources of considerable separation and so of additional drag, as will be shown later on.

b) Comparison of axial-flow calculation with measurements on free-running radiators.- Linke and Friedrichs (reference 4) made some axial flow and drag measurements on free-running radiators, with systematic changes in inlet and exit opening. The internal drag of the core was simulated by screens, by means of which the most varying permeabilities (i.e., percentage of open area in radiator) could be reproduced.

The test results together with the values obtained by means of equation (3a) are plotted in figure 12. They prove that the upper limit of flow is actually governed by the diffuser opening ratio $F_3/F_2$ alone. The test values hug the computed curves very closely as long as the diffuser orifice ratio exceeds that of the nozzle.* This is particularly apparent for ratio "H 15" where all test values for diffuser orifice ratio greater than the nozzle orifice ratio, are almost exactly on the computed curve. Not until the diffuser orifice ratio falls below that of the nozzle orifice is there any perceptible drop in flow, as, for instance, for "V 13."

It is again stressed at this point that the drop in flow due to narrowing the diffuser to less than that of the nozzle, is solely attributable to the severe diffuser losses evidenced in the marked rise of radiator drag (see section B,I,2a and 2b), which in effect is equivalent to

*A partial explanation of the discrepancy between the computed and experimental values in the zone of low core permeability is that, as the rate of flow decreases the permeability of the screens decreases also.

the higher pressure drop of a less permeable core. From this point of view, it is even possible to compute the diffuser drag from the drop in axial flow coefficient.

To prove the correctness of this reasoning, the following example is cited:

On switching from duct V 66-H 65 to V 36-H 65 while using the same screen, there was a material drop in axial flow; for instance, at $\eta_{ai} = 0.72$, according to figure 12. If this reduction is really attributable to the higher diffuser losses alone - that is, equivalent to a decrease in the permeability of the screen to $\eta_{ai} = 0.466$ with the same ducts V 66-H 65, then the total drag with this reduced screen permeability and favorable diffuser ducts must itself be equal to the total drag of the unfavorable system V 36-H 65. And the recorded drag plotted in figure 14 actually shows both radiator systems to have a drag coefficient of $c_w = 0.32$. Accordingly, the change from diffuser orifice V 66 to the adverse V 36 has the same effect as a rise in pressure-drop coefficient $c_{wk}$ of the screen from 0.92 (corresponding to $\eta_{ai} = 0.72$) to 3.6 (corresponding to $\eta_{ai} = 0.466$). And the same relationship holds for other test points between diffuser loss and flow decrease, according to a subsequent check.

The conclusions drawn from this comparison are:

Regulation of flow through radiator: So long as there is no separation of flow from the diffuser wall, this flow can be regulated only by adjustment of the radiator exit valves; in separation free flow, an adjustment of the inlet valve is ineffective as far as the flow volume is concerned.

At low flying speed, as in climb, for instance, a too-narrow diffuser may cause such pronounced separations within the diffuser that further opening of the exit valve does not afford the necessary increase in the comparative air flow in respect to high speed - in which case the effect of the exit valves can be noticeably improved by opening the inlet valves.

Prediction of radiator flow: With proper ducts (i.e., correct size of diffuser) and given percentage of open area of radiator core, the flow through a free-running radiator can be accurately enough computed from equation (3a). The

premise of pressure of free flow at diffuser exit is amply complied with, even with short radiator ducts.

For built-in radiators, even if of the belly type, the flow could be ascertained from equation (3b), provided the difference between the pressure at radiator exit and that of undisturbed free flow is known. However, this difference is generally not assessable with wind-tunnel tests, since the prediction of the effect of pressure distribution of the free flow through the radiator is usually impossible. For these reasons, it is recommended that the flow through built-in radiators be established by experiment.

## 2. Drag of Unheated Radiators

a) Calculation of cooling drag.- The internal drag of a ducted radiator, termed "cooling drag" hereafter, is composed of the drag in the core and the pressure forces on diffuser and nozzle in separation-free stream. The cooling drag represents herein the minimum drag of a ducted radiator in free stream (in contrast to the positive ventilated radiators) which may be spent for heat dissipation under the existing conditions of cooling, such as frontal area of radiator, type of core, temperature of cooling agent, air density, etc. Both the pressure drop within the core and the pressure forces on diffuser and nozzle are inseparably associated with a radiator in free stream. For instance, the cooling drag would also be created, even if a radiator could be so mounted in a certain airplane that the installation required neither enlargement of the outside surfaces - hence of the friction drag of the airplane - nor created flow interference about the other parts of the airplane as, for instance, by eddy separation or adverse boundary-layer influence.

In general, the diffuser exerts a drag-decreasing pressure force, and the nozzle a drag-increasing pressure force. In their entirety, diffuser and nozzle forces yield a drag-decreasing component if the nozzle exit orifice is equal to or less than the radiator frontal area.

The cooling drag of the unheated radiator can be determined by Weinig's method, which is briefly discussed here.

The total drag $W$ of the ducted radiator must equal the loss of momentum of the air flowing through the radiator, i.e.:

$$W = \frac{G}{g} \Delta v = F_k \, v_o \, \eta_{ae} \, \rho \, (v_o - v_3)$$

(fig. 9), with $G$ the weight of air per second.

Then the drag coefficient of the ideal ducted radiator $c_w = \frac{W}{\rho/2} v_o^2 F_k$ follows as $c_w = 2 \eta_{ae} \left(1 - \frac{v_3}{v_o}\right)$, leaving unknown the velocity ratio $v_3/v_o$ for a given radiator installation. But this is readily obtainable from the energy equation, as the energy loss between the sections $F_o$ and $F_3$ must equal the energy loss between $F_1$ and $F_2$ (diffuser and nozzle losses as well as wall friction on diffuser and nozzle are disregarded) and consequently, is solely represented by the energy loss in the actual core:

$$\frac{v_o^2}{2g} + \frac{p_o}{\gamma} = \frac{v_3^2}{2g} + \frac{p_o}{\gamma} + c_{wk} \frac{v_1^2}{2g}$$

Computing the velocity ratio $v_3/v_o$ from this equation ultimately affords as cooling-drag coefficient $c_w$ of the unheated built-in radiator without diffuser and nozzle losses:

$$c_w = 2 \eta_{ae} \left(1 - \sqrt{1 - c_{wk} \eta_{ae}^2}\right) \qquad (4)$$

The thus-defined internal cooling drag is equally valid for the built-in radiator which generally has, at nozzle exit, a pressure other than that of the undisturbed free stream. The cooling drag is supplemented by other drag caused by wall friction on the inside and outside surfaces of the radiator, by influencing the flow around the other parts of the airplane as well as by eddy drag, for instance, as a result of separations on the diffuser. It is important, then, to establish the relation between the measured radiator drag in relation to the theoretically defined drag, and also the extent of the individual drag sources on the total radiator drag.

b) Comparison of recorded drag on free-running radiators with the computed minimum drag (equal frontal radiator area).- To this end the systematic test series of Aachen Aerodynamic Institute on free-running radiators (reference 4) was again resorted to. The measured drag coefficients were plotted in figures 13 to 16. The cool-

ing drag was computed from equation (4) on the basis of the measured axial flow ratio $\eta_{ae}$ (cf. L 4) which, by separation-free radiator covering agrees with that computed according to equation (3a). (Cf. section B,I,1b.)

Corresponding to the limit value for aerodynamic surfaces at medium Reynolds Number of tunnel tests (Re ~ $3.5 \times 10^6$), the local friction coefficient of the outside surfaces was put down at $c_f = 0.003$. The velocity increases on the outside surfaces, as a result of the displacement effect of the radiator, were allowed for according to Eick (reference 12) by a percentage increase over that of flat-plate friction which, for the completely closed, streamlined ducted radiator, amounted to ~ 25 percent. Since the velocity increases created by the resistance body decreases with increasing permeability of the radiator installation and ultimately disappear for unrestricted flow ($\eta_{ae} = 1$), the proportionate increase of friction drag for the different flow coefficients was interpolated according to the following formula:

$$\frac{\text{Percent increase of friction coefficient at } \eta_{ae}}{\text{Percent increase of friction coefficient at } \eta_{ae} = 0} = 1 - \eta_{ae}$$

With the thus-obtained coefficient the drag of the outside surfaces could be computed for any opening ratio.

The drag coefficient on the inside surfaces was again put at $c_f = 0.003$. Conformable to the assumption of incompressible fluids, the velocity at the different points is determined by the section ratio, hence leaving for the friction-pressure decrease $\Delta p_{ri}$ on the inside surfaces of the ducts, the following coefficient:

$$\frac{\Delta p_{ri}}{\frac{\rho}{2} v_o^2} = \Delta c_{w_{ri}} = c_f \eta_{ae}^2 \int_0^{l_d} \left(\frac{F_k}{F_x}\right)^2 \frac{U_x}{F_x} \, dx$$

(See fig. 17.) $U_x$ = inside circumference of diffuser at point x.

The integral in this equation was graphically determined for every single duct.

The computed values for the radiator drag - i.e., the internal cooling drag - in addition to the friction drag at the inside and outside surfaces together with the test values, are shown in figures 13 to 16. Whereas the friction drag on the outside surfaces increases in significance as $\eta_{ae}$ decreases (i.e., as the nozzle-orifice ratio diminishes), the friction drag of the inside walls is, as a result of the low velocity, so small, on the whole, that it can be ignored. Fundamentally, the computed values are in quite close agreement with the test values so long as the diffuser orifice ratio remains below that of the nozzle. For such radiator ducts therefore the diffuser and nozzle loss remains a negligible proportion of the total loss. Even for the pronounced sectional enlargement on diffuser "V 36" the diffuser loss remains within measuring accuracy if the nozzle, for instance, up to orifice ratio "H 15" is closed. Contrariwise, as soon as the diffuser orifice ratio falls below that of the nozzle, the losses are severe, as plainly seen on nozzle "H 65" at transition from "V 66" to "V 36" in figure 14. While for diffuser "V 66" the test values still coincide with the mathematical, on switching over to "V 36" at around the core permeability, equivalent to a change from too-narrow to too-wide diffuser, the measured drag manifests a sudden rise.. This rise cannot be ascribed, say, to increased vortex formation at the nozzle exit, and for the following reason: At exit from the radiator when using the same nozzle the vorticity is solely dependent upon the difference between the speed of the free stream and that emerging from the radiator - i.e., the added drag on the radiator exit is in this case solely a function of $\eta_{ae}$. At $\eta_{ae}$ values, as for diffuser "V 36" the covering "V 66-H 65", however, manifests practically no nozzle or diffuser losses, hence the exit losses with covering "V 36-H 65" must be negligibly low. And the sudden rise in radiator drag on the previously cited change to diffuser "V 36" is, in consequence, largely attributable to flow separation within the diffuser, as explained in figure 11, for two narrow diffusers.

A diffuser as short as possible, so as to surely prevent separations within the diffuser, is accordingly propitious for radiator ducts.

The lower limit of diffuser length, set by the danger

of flow separation on the outside of the diffuser, can be prevented by care in the design of the entrance orifice.

A further advantage of the shortened diffuser lies in the reduced friction-afflicted surfaces, especially the outer radiator walls, whose friction drag rises as the flow decreases; i.e., as the nozzle orifice ratio is smaller. At high-speed flight, particularly where the average $\eta_{ai}$ range between 0.4 and 0.5, and the $\eta_{ae}$ at around 0.2 (approximately corresponding to the nozzle orifice ratio "H 34"), the friction drag on the outside radiator wall is of the approximate order of magnitude of the internal cooling drag. On high-speed aircraft this division should shift to even greater proportions of friction drag to total drag, since at high speed the optimum $\eta_{ae}$ tend toward values which are even less than $\eta_{ae} = 0.3$. From this large share of the external friction drag it can be concluded, in accord with a study by Kramer in the DVL, that the freely exposed radiator must be inferior to that mounted in the airplane, provided detrimental effects in both cases are avoidable. Long air passages for guiding the air from air inlet to the core, can be readily admitted, since this air guidance can be effected at low speed, i.e., low losses. In short, it can be concluded from the comparison, that drag and flow on freely exposed radiators are accurately enough predictable if stream separations on the radiator ducts, especially on the diffuser, are avoided.

## II. THE HOT RADIATOR

Heating increases the pressure drop in the core, as already pointed out. This increase in pressure drop, which on a ducted radiator results in increased drag with rising heat, is confronted by the favorable effect of heating on the pressure exerted by the radiator duct. As a result of the greater volume due to heating, the air leaves the core at greater velocity than from the cold core. According to the law of momentum, there must therefore be an additional force (compared to the cold radiator) which lowers the drag of the ducted radiator. But this additional beneficial force through heating, can be transferred to the radiator ducts only by a change in the pressure forces, as explained in the following comparison of radiators with equal air induction in hot and cold stages:

Case 1: On emergence from the core a positive pressure prevails relative to free flow (high speed). There always is, as known, a drag-decreasing pressure on the diffuser, and a drag-increasing pressure on the nozzle, as shown in sketch 1. If the pressure drop in the core is increased by mounting a less permeable cold core (sketch 1b), by identical air flow, the streamline pattern before the diffuser and hence the diffuser force itself, remains the same. But the nozzle must be opened wider to insure the pressure of free flow on emergence from the nozzle. Opening the nozzle lowers the adverse nozzle force, which ultimately disappears when the nozzle is wide open; as a result, part of the higher drag in the core is made ineffective by mounting a less permeable core.

Heating the radiator (sketch 1c) does not change the diffuser force by identical air flow. Since, however, the kinetic energy of the emerging air stream rises as a result of heating,

$$E_T \sim \rho_T v_T^2 = \frac{T_o}{T_1} \rho_o \left(\frac{T_1}{T_o}\right)^2 v_o^2 = \frac{T_1}{T_o} E_o$$

(increased pressure drop in core due to heating is disregarded), the nozzle should not be throttled as much as on the cold radiator, so as to insure, on emergence, the pressure of free flow. Hence there is a drag-decreasing force.

The increased drag of the core due to heating is faced by the favorable reaction of the heating on the nozzle force, created by the heightened pressure drop as well as by the higher kinetic energy of the air stream.

Case 2: Negative pressure relative to free flow (climb) on emergence from the core (sketch 2).

As before, the diffuser exerts a drag-decreasing, and the nozzle a drag-increasing effect. By reducing the core permeability (cold, sketch 2b), the diffuser force remains the same by equal air flow, although the nozzle must be opened wider and as a result a greater drag-increasing nozzle force is now created. Owing to the higher energy content of the emergent hot air (sketch 2c) the nozzle, by equal air flow (increased pressure drop in core due to heating is disregarded), can be throttled more so that as before, a decrease in the adverse nozzle force is produced. From the superposition of these two separate effects, it

can be inferred, for the heated radiator, that in case 2, the heightened drag of the heated core is still further increased by the reaction of the greater pressure drop on the nozzle force; only the higher kinetic energy of the heated air stream on emergence from the radiator affects the nozzle force in a drag-decreasing sense.

Depending upon the heating condition and the data for a radiator whose air flow is kept the same, hot or cold, the increase in core drag on heating, or the favorable reaction of the air expansion on the nozzle force, preponderates; hence the heated radiator may disclose a drag which is higher or lower than the cold radiator, depending upon the particular case.

In the numerical treatment of the drag of cold radiators, it may again be assumed that the air in diffuser and nozzle is incompressible, although the air density in diffuser and nozzle may be different, in accord with the heating in the core. For the actual core the air density must be considered variable, as shown in simple approximations, with assumedly known thermal efficiency $\eta_{th}$ and drag coefficient $c_{wk}$ of cold core, as known from the conventional core measurements.

## 1. Flow through Hot Radiator

Separating the two chief heat effects - increased pressure drop in core and gain of energy in emergent air - the air volume must decrease as the heat increases as a result of the lowered permeability of the heated core, unless the orifice ratio of the nozzle is modified accordingly. On the other hand, the gain in kinetic energy lowers the flow only if the orifice ratio $F_3/F_2$ of the nozzle is less than 1; contrariwise, the flow increases if, as usual in climb, the nozzle operates as diffuser ($F_3/F_2 > 1$). (Compare sketches 1 and 2.)

a) Necessary enlargement of nozzle orifice by equal flow.- If, in a wind-tunnel test on an airplane with cold radiator, the predetermined flow velocity is controlled by corresponding opening of the radiator shutters, on the heated radiator the exit flaps must, in general, be opened wider than on the cold radiator to produce the same air flow and consequently, the required heat dissipation in the heated stage. This effect of the radiator heating cannot be perfectly copied in a model test with cold radiator,

where, to be sure, the higher pressure drop of the heated radiator can be simulated by corresponding reduction in permeability in the model radiator core, but not the effect of the greater volume of heated air. Consequently, in order to establish the required increase in nozzle orifice ratio the test with cold core must be supplemented by flow calculations, such as equation (3). For the hot radiator, equation (3a) reads:

$$\eta^{+2}_{ae_T} = \frac{1}{1 + c^{+}_{wk_T} + \frac{T_2}{T_1}\left(\frac{f^2 F_2^2}{F_{3T}^2} - 1\right)}$$

To insure the same coefficient of flow for the hot and the cold radiators the nozzle of the heated radiator must be opened wider in the following ratio:

$$\frac{F_3^2}{F_{3T}^2} = \left[\frac{F_3^2}{f^2 F_2^2} + \frac{T_1}{T_1 + \eta_{th}(T_w - T_1)}\left(1 - \frac{F_3^2}{f^2 F_2^2}\right)\right]$$

$$-\left(\frac{F_3^2}{f^2 F_2^2}\right) f^2 c_{wk} \frac{\eta_{th}(T_w - T_1)}{T_1 + \eta_{th}(T_w - T_1)}\left[\frac{5}{8}\left(1 + \frac{1}{6}\eta_{th} + \frac{1}{12}\eta_{th}^2\right) + \frac{2}{f^2 c_{wk}}\right] \quad (5)$$

Here the first term allows for the greater exit volume of air due to heating, while the second term indicates the change in nozzle opening as the result of heightened pressure drop in the radiator. The equation is also applicable to built-in radiators; for instance, for belly radiators, since the positive or negative pressure of free flow existing at nozzle exit is effective for the cold as well as for the hot radiator, and cancels in the calculation.

b) Flow reduction due to heating by equal nozzle orifice.- If the nozzle opening on the heated radiator remains the same as on the cold radiator, a drop in flow will result for the reasons cited above. This, at the same time changes the characteristic values of the corresponding cold radiator which, for minor flow change, can

be accurately enough gaged from the following.

The pressure-drop coefficient of the cold radiator is (reference 8):

$$c_{wk_{(T)}} = c_{wk}\left(\frac{\eta_{ae}}{\eta_{ae_T}}\right)^{0.25}$$

The thermodynamic efficiency for minor change is (reference 9):

$$\eta_{th_{(T)}} = \eta_{th}\left(\frac{\eta_{ae}}{\eta_{ae_T}}\right)^{0.21}$$

With these values the ratio of flow coefficient for cold and hot radiator with equal radiator ducts can be computed according to equation (3a):

$$\eta_{ae_T} = \eta_{ae}\sqrt{\frac{1}{1+A}} \qquad (6a)$$

whereby

$$A = \eta_{ae_T}^2\left\{c_{wk}\left[\left(\frac{\eta_{ae}}{\eta_{ae_T}}\right)^{0.25} - 1\right] + \right.$$

$$+ \frac{\eta_{th_{(T)}}(T_w - T_1)}{T_1}\, c_{wk}\left(\frac{\eta_{ae}}{\eta_{ae_T}}\right)^{0.25}$$

$$\left[\frac{5}{8}\left(1 + \frac{1}{6}\,\eta_{th_{(T)}} + \frac{1}{12}\,\eta_{th_{(T)}}^2\right) + \right.$$

$$\left. + \frac{2}{f^2\, c_{wk}\left(\frac{\eta_{ae}}{\eta_{ae_T}}\right)^{0.25}}\right]$$

$$\left. + \frac{\eta_{th_{(T)}}(T_w - T_1)}{T_1}\left(\frac{1}{\eta_{ae}^2} - \frac{1}{f^2} - c_{wk}\right)\right\} \qquad (6b)$$

This equation is also accurate enough for built-in radiators since in it the pressure difference of the free flow is contained only in a term of little import. Graphical presentation of this relationship was not deemed worthwhile as the practical importance of this equation is slight; the case of equal flow velocity with corresponding setting of radiator shutters is generally more important.

## 2. Drag of Heated Radiator

a) Cooling drag.- The cooling drag must be equal to the loss of momentum of the air flowing through the radiator; i.e., the following fundamental equation retains its validity for the heated radiator also:

$$c_{w_T} = 2\,\eta_{ae_T}\left(1 - \frac{v_{3T}}{v_0}\right) \tag{7a}$$

Then the energy equation, by assuming loss-free energy conversion in diffuser and nozzle and separation-free flow, gives the velocity ratio $v_{3T}/v_0$. The energy loss must, according to the stipulated assumptions between sections 0 and 3, be of the same order of magnitude as between sections 1 and 2 (fig. 9). For sections 1 and 2, the solution of the energy loss involves no difficulties since, according to section A,III,1, the heightened pressure loss due to heating, as well as the velocity and air density at radiator entry and exit are known:

$$\frac{v_0^2 - v_{3T}^2}{2g} + \left(\frac{p_0}{\gamma} - \frac{p_0}{\gamma_T}\right) = \frac{v_1^{+2} - v_{2T}^{+2}}{2g} + \frac{p_1^+}{\gamma} - \frac{p_1^+ - c_{wk_T}^+ \frac{\rho}{2} v_1^{+2}}{\gamma_T}$$

or

$$\frac{v_0^2 - v_{3T}^2}{2g} = \frac{v_1^{+2} - v_{2T}^{+2}}{2g} - \frac{p_1^+ - c_{wk_T}^+ \frac{\rho}{2} v_1^{+2}}{\gamma_T} + \frac{p_1^+}{\gamma} - \frac{p_0}{\gamma} + \frac{p_0}{\gamma_T}$$

$$= c_{wk}\frac{v_1^2}{2g} + \varphi_T \frac{v_0^2}{2g} \tag{7b}$$

The quantity $\varphi_T$, which characterizes the heating effect, is determined as follows:

$$\varphi_T = \eta_{ae_T}^2 \frac{\eta_{th}\,(T_w - T_1)}{T_1} \left\{ c_{wk} \left[ 1 + \frac{5}{8} \left( 1 + \frac{1}{6}\,\eta_{th} + \frac{1}{12}\,\eta_{th}^2 \right) \right.\right.$$

$$\left.\left. \times \left( 1 + \frac{\eta_{th}\,(T_w - T_1)}{T_1} \right) \right] - \left[ \frac{1}{\eta_{ae_T}^2} - \frac{1}{f^2} \left( 1 + \frac{\eta_{th}\,(T_w - T_1)}{T_1} \right) \right] \right\} \tag{8a}$$

The change in velocity head of the air flowing through the radiator is, in this concept, divided into two parts: one part corresponding to the energy loss of the cold radiator, and the other part containing all effects of heating. The second, additional part following the core heating can be positive or negative - therefore deciding whether the heating creates a reduction ($\varphi_T < 0$) or an increase ($\varphi_T > 0$) in radiator drag. Solving the velocity ratio $v_{3T}/v_0$ from equation (7b) and inserting the obtained value in equation (7a), the cooling drag of the heated radiator follows as:

$$c_{w_T} = 2\,\eta_{ae_T} \left( 1 - \sqrt{1 - (c_{wk}\,\eta_{a_T}^2 + \varphi_T)} \right) \tag{8b}$$

For rapid solution of quantity $\varphi_T$ the chart, figure 18a, for great air heating, and chart, figure 18b, for small air heating, were made. The curves for $\varphi_{T_1}$ indicate the effect of increased pressure drop in the core*, and the $\varphi_{T_2}$ curves indicate the effect of air expansion on the acceleration pressure drop in the core and on the nozzle force. If $\varphi_{T_1}$ exceeds $\varphi_{T_2}$, the heating induces a rise in drag. If, on the other hand, $\varphi_{T_2}$ exceeds $\varphi_{T_1}$ the heating lowers the cooling drag. In consequence, the following case may fundamentally arise:

---

*On the $\varphi_{T_1}$ curves the expression $\left(1 + \frac{1}{6}\,\eta_{th} + \frac{1}{12}\,\eta_{th}^2\right)$ was computed for $\eta_{th} = 0.5$, because of the smallness of $\eta_{th}$. The error in the ordinate of the $\varphi_{T_1}$ curves, for instance, amounts - at $\eta_{th} = 0.75$ - to only 3 percent for a sea-level temperature difference of around 200° C., and becomes less as the temperature differences decrease.

1. By great pressure-drop coefficient $c_{wk}$ of the cold core, and great flow coefficient $\eta_{ae}$, the heating always creates a rise in cooling drag.

2. By small pressure-drop coefficient $c_{wk}$ for the cold core and correspondingly low flow coef $\eta_{ae}$, the radiator drag decreases at first in increasing measure as the heating increases. But, beginning with a certain temperature, the reduction in radiator drag decreases until, by further increasing heat, the drag of the hot radiator is greater than that for the cold radiator.

Naturally the rise in radiator drag through heating occurs only when the drag of the cold radiator of equal $\eta_{ae}$ is to be concluded from the drag of the heated radiator. On the other hand, increasing the heat oi a radiator with given heat dissipation - say, by changing from water cooling to high-temperature liquid cooling - the drag will, of course, drop, according to equation (8b) since either - with equal core - the flow coefficient or by equal flow coefficient the size of the core could be reduced. Chart (fig. 19) is designed for the determination of the drag difference $\Delta c_w$ of cold and heated radiator, whose flow is maintained even by proper adjustment of the shutters:

$$\Delta c_w = c_{w_T} - c_w$$

$$= 2\,\eta_{ae}\left(\sqrt{1 - c_{wk}\,\eta_{ae}^2} - \sqrt{1 - (c_{wk}\,\eta_{ae}^2 + \varphi_T)}\right)$$

It affords the additional drag in simple manner, for instance, the amount to be added to the drag with unheated radiator in the wind tunnel, in order to obtain the drag of the heated full-scale version. This change in internal cooling drag due to heating holds for freely exposed, as well as for built-in radiators; however, it should be noted that the heated cooling stream may create a change in additional drag which, for example, must be attributed to influence of the boundary-layer formation on the other parts of the airplane or to intermingling of the emerging cooling air stream with the free stream. (See sec. B,III.)

b) Comparison of theory and test for freely exposed radiators.- The Aachen Aerodynamic Laboratory made a series of tests on various freely exposed radiators with systematically changed inlet and outlet orifices in cold and heated stages, whereby the heating of the radiator wall in respect to the entering air was expanded up to temperatures of over 100° C. (reference 4). In these measurements the air speed and radiator-shutter setting remained the same in the cold as in the heated stage, hence the heated radiator (sec. B,II,4) disclosed a lower flow coefficient than the corresponding cold radiator. The measurements included the heat dissipation of the radiators, the rise in air temperature on flowing through the core, and the drag reduction of the heated versus the cold radiator.

From the data for heat removal and air temperature rise, the flow coefficient was derived. The curve of the flow coefficient for different degrees of heating was then extrapolated to zero heat, and with this extrapolated value the flow reduction due to heating computed for the unheated radiator. Then the recorded flow reduction was compared with the theoretical results from equation (6). But the results did not agree, although the discrepancies were small; for instance, the 3-percent air-temperature rise, which was due to a mistake in measuring. However, since in this order of magnitude the range of errors in temperature measurement must be looked for, these test data afford no reliable basis for a check.

The reduced drag due to heating can, however, be much more accurately measured than the mean air-temperature rise; first, because the discrepancies are greater, and second, the accuracy of weighing exceeds that of the temperature recording. The reduced drag due to radiator heating was computed with equation (8), whereby the reduction in flow was ascertained from equation (6). The results are plotted in the same manner together with the test points as in the Aachen Laboratory (fig. 20). Here theory and test are in fairly accurate agreement; varyingly high heating shifts the curve in very little measure, hence the test points are practically on one curve.

This comparison proves that, up to 100° C. temperature of radiator heating, the derived formulas reproduce the effect of heating on the radiator drag quite well.

c) Comparison with Weise's radiator theory for very high heating (reference 7).- A. Weise made a theoretical analysis of the energy conversion in heated radiators. He computed, as special case - i.e., for radiator installations without nozzle with radiator cores, which closely approach the ideal case of core $\Omega = 1$, according to Weise) - the internal cooling drag, and published it in figure 8 of the cited report. The temperature of the radiator wall was increased to ten times the air inlet temperature - i.e., on the ground, up to radiator heating of around 3,000° Abs. His criterion for radiator drag was a quantity $\Omega_e$ which ties in with the values of the present report through

$$\Omega_e = \frac{1}{\eta_{th}} \left(1 - \sqrt{1 - \left(c_{wk}\, \eta_{ae_T}^2 + \varphi_T\right)}\right) = \frac{c_{w_T}}{2\, \eta_{ae_T}^2\, \eta_{th}}$$

For comparison we then computed, for equal temperature difference, the internal cooling drag with the approximate equations (1), (3a), (8a), and (8b), and plotted the results along with Weise's data in figure 21. As connection between pressure-drop coefficient $c_{wk}^{+}$ and thermodynamic efficiency $\eta_{th}$ of the core, we used the values of the heated single tube (equivalent to ideal core), according to figure 2, whereby the pressure-drop coefficients of the single tube were multiplied by 1.12, in correspondence with Weise's efficiency factor $\Omega = 1$ (reference 7, fig. 4).

The comparison is satisfactory even for such unusually high degrees of heating as 3,000° (corresponding to $\xi = \frac{T_w}{T_1} = 10$). (Minor discrepancies might be attributed to slightly deviating assumptions for the single tube, fig. 2.) Thus, the use of the test data for $c_{wk}$ and $\eta_{th}$ of the single tube (fig. 2) yields the same results as the coupled introduction of these values in the shape of Weise's $\Omega$. Even the approximated change in pressure drop due to heating has no noticeable effect, so that the working charts can be accurately enough applied to the heating effect in radiators in all practical cases, including exhaust-gas coolers.

## III. THE BUILT-IN RADIATOR

In the foregoing, the theoretical and experimental radiator drag on freely exposed radiators was compared,

and good agreement obtained for separation-free radiator ducts. The problem now is to establish the extent of this agreement for built-in radiators and sources of additional drag above the minimum.

1. Comparison of Theory and Test for Built-in Radiators

Two different belly-type radiators were tested at full scale in the DVL wind tunnel by Schlupp (not published), with the cores heated to temperature differences of 57° C. between mean cooling-fluid temperature and air-inlet temperature (figs. 22 and 23). The flow velocity and hence, the internal cooling and friction drag were deduced from the measured heat dissipation and the characteristic values of the employed radiator systems. The skin friction drag on the ducts was estimated by means of the additional outside surface and an assumed friction coefficient of $c_f = 0.003$.

The comparison disclosed agreement in both values at high flow coefficients, as in climbing, up to discrepancies of around ±30 percent, while at low flow coefficients of high-speed flight ($\eta_{ae} < 0.2$), the internal cooling drag and the friction drag amounted to but a small fraction of the measured total drag. This additional drag at low $\eta_{ae}$ rises considerably with largely closed inlet opening of the diffuser, and so confirms the statement made in section B,I,2.

For comparison, we quote further from several unpublished test data of tests made in the small DVL wind tunnel by Zobel, on elongated bodies of different aspect ratio, in whose forebody different radiator systems were simulated by means of unheated screens (fig. 24), although these measurements cannot be fully evaluated for comparing the installation conditions of real radiators. The investigations disclosed that at high $\eta_{ae}$ the measured drag was less than the theoretical and vice versa. The drag proportion exceeding the minimum drag in the range of small $\eta_{ae}$ of high-speed flight, is more than half as small as on the cited belly radiators (figs. 22 and 23). A systematic effect of the fineness ratio of the body behind the radiator could not be gleaned from the measurements.

The discrepancy between calculation and measurement

is primarily attributable to the following causes:

1. Separation losses, especially by unsteady transitions after adjustment of control flaps.- On the explored belly radiators, for instance, the contour line of the built-in radiator forms a bend at the transition from rear control flap to core, which becomes sharper as the flow decreases. The outside flow has a tendency to separate at this point. If this happens, the whole flow on the bottom side of the fuselage is impaired - probably creating severe additional losses.

2. Effect of radiator wake on the fuselage drag.- The air through the radiator emerges at higher temperature and, depending on the degree of heating, at lower or higher velocity than the free stream. The air viscosity is higher as a result of the temperature rise, causing the wall friction of the airplane components exposed to the radiator wake to increase. Following the changed velocity in the radiator wake, the exposed areas of the airplane are subject to a different velocity than in free air stream. By greatly slowed-down radiator wake (i.e., high $\eta_{ae}$), the friction drag therefore would decrease, and by accelerated radiator wake (for instance, by highly heated radiator and small $\eta_{ae}$), increase. This would explain the shape of the curves in figures 23 and 24, which the test curves assume at high $\eta_{ae}$ below the minimum drag. On the other hand, the radiator wake might create a flow effect similar to that produced by an auxiliary airfoil on a wing. For, like an auxiliary airfoil, the radiator wake with increased velocity can accelerate the boundary layer, and so postpone the separation. A slowed-down radiator wake, which would retard the boundary layer still more and so promote separation, would, of course, have the opposite effect.

The described effects are decisively dependent upon whether the velocities in the radiator wake exceed or fall below the velocity of free flow. For pressure of free flow at radiator exit* the velocity ratio in the radiator wake is:

$$\frac{v_{s\,T}}{v_o} = \sqrt{1 - (\eta^2_{ae_T}\, c_{wk} + \varphi_T + \Delta c_{w_{ri}})}$$

*If there is a certain pressure difference on the radiator exit in respect to the pressure of free flow, the velocity at the radiator exit can be computed with the aid of Bernoulli's equation.

($\varphi_T$ from figs. 18a and 18b). In one example, worked out with this equation (table II) for high-speed flight, it resulted in a velocity increase at the radiator exit, even if a core of modern quality with high-temperature liquid cooling was employed.

If the effect of the wake constitutes the primary cause of the drag discrepancy between theory and test, it follows that all radiator drag measurements must - to be transferable - be effected on the heated radiator, since at high-speed flight the heating exerts a substantial effect upon the wake.

TABLE II

Division of Minimum Radiator Drag on the Exemplary Airplane at High Speed (Belly Radiator)

| Cores | Coefficient of drag components (referred to $F_k$) | | | | Total drag coefficient | |
|---|---|---|---|---|---|---|
| | Cooling drag | Internal friction | Skin friction | Heating $\Delta c_w$ | Cold $c_w$ | Heated $c_{w_T}$ |
| Ideal core $c_{wk}$= 2.3; $\eta_{th}$=0.70 | 0.0093 | 0.0001 | 0.0159 | -0.0392 | 0.025 | -0.014 |
| Modern quality core $c_{wk}$=6.0; $\eta_{th}$=0.70 | 0.0242 | 0.0001 | 0.0159 | -0.0333 | 0.040 | +0.007 |

3. Pressure distribution changes due to the intermingling of air from the radiator with the free stream - (stressed by Weise in the DVL).- The air, on emerging from the radiator, usually has a different velocity than the free stream, so that on the free boundaries of the emerging air flow, mixes with the other air. Now, if this mixing with the outside air takes place at a pressure greater or smaller than the pressure of the free stream, the pressure field changes and, with it, the drag of (radiator + fuselage).

To what extent the different effects contribute to the difference between computed and measured total radiator

drag, it is impossible to find out with the available test data. If the different effects combine to make the reaction of the cooling air on the exposed airplane components favorable, the radiator will preferably be so disposed that a large portion of the airplane surfaces will be washed by the radiator wake; otherwise, as little area as possible will be exposed - which might, for instance, be accomplished by guiding the cooling air in channels as far as the trailing edge of the wing or body. The internal friction drag could be low quite easily, as the air can be conducted with low velocity. The aim of further research on built-in radiators therefore, will be to establish the causes of the additional drag and find ways to avoid them.

## 2. Comparison of Minimum Drag with Actual Drag of Radiators Mounted on Aircraft

With a view to attesting the practicability of the obtained relations and a survey for different radiator mounting systems, of the ratio of the minimum radiator drag in actual airplanes, the radiator drag was determined on an airplane having the following data (additional drag due to separation of flow, boundary-layer effect, mixing of air, etc., disregarded):

| | |
|---|---|
| Horsepower | $N = 2 \times 1{,}000$ hp. |
| Speed at 4,000 m | $v = 470$ km/h |
| Heat to be removed in radiator | $Q = 2 \times 320{,}000$ kcal/h |
| Frontal area of radiator | $F_K = 2 \times 0.27$ m$^2$ |
| Temperature difference between radiator wall and incoming air (high-temperature liquid cooling), | $T_w - T_1 = 115^\circ$ C. |

Assuming a core with $\eta_{th} = 0.70$ thermodynamic efficiency, which is equivalent to optimum, the flow coefficient $\eta_{ae\overline{T}}$ follows from the heat removal at

$$\eta_{ae_T} = \frac{Q}{c_p (\gamma F_k v) \eta_{th} (T_w - T_1)} = 0.159$$

The calculation was made once with an ideal core ($c_{wk}$ = 2.3; single-tube curve, fig. 2), and then with a core of present-day efficiency ($c_{wk}$ = 6.0; f = 0.75) to bring out the effect of the core. The pressure drop was assumed to be more than twice as high in respect to the ideal core. The radiators are slung as belly radiators under the engine nacelles. Then the outside area of the belly radiator is that additionally needed by the radiator - i.e., essentially only the two side walls of the radiator ducts, including the radiator step; in this case, 1.4 $m^2$ per radiator (table II).

The minimum drag of the belly radiator is greatly lowered by the heating so that with the ideal core a slight forward speed occurs and on the core of present-day efficiency, only a disappearingly small drag remains. Since the radiators in actual airplanes manifest average drag coefficients of between $c_w$ = 0.5 and 0.2 in high-speed flight, all the computed drag components are of a 10-percent lower order of magnitude.

The causes of higher drag of real radiators over the computed minimum values have been previously discussed. Consequently, if the aim to build in a radiator without creating additional drag succeeds, it will practically eliminate the total radiator drag - which, in high-speed flight is equivalent to a saving of from 5 to 10 percent in the total driving power of the airplane.

With the freely exposed radiator, of course, additional drag is comparatively easy to avoid, as shown in the wind-tunnel tests (figs. 13 to 16). But this saving in drag is partially neutralized again by the drag of the larger outside areas. The drag coefficients for the freely exposed radiator with circular section (same frontal area as the belly radiator) are given in table III.

In spite of the greater surfaces, the freely exposed radiator is, at present, substantially superior to the belly radiator. The best drag coefficients obtained up to now with belly radiators are still about twice as high as the figures for the freely exposed type computed in table III which, without appreciable additions, are equivalent

to the experimentally obtained figures (13 to 16).

TABLE III

Division of Minimum Radiator Drag on the Exemplary Airplane at high speed (freely exposed jet-type radiator)

| Cores | Coefficient of drag components (referred to $F_k$) | | | | Total drag coefficient | |
|---|---|---|---|---|---|---|
| | Cooling drag | Internal friction | Skin friction | Heating $\Delta c_w$ | Cold $c_w$ | Heated $c_{w_T}$ |
| Ideal core $c_{wk}$= 2.3; $\eta_{th}$=0.70 | 0.0093 | 0.0004 | 0.0892 | -0.0392 | 0.099 | 0.060 |
| Modern quality core $c_{wk}$=6.0; $\eta_{th}$=0.70 | 0.0242 | 0.0004 | 0.0892 | -0.0333 | 0.114 | 0.081 |

In both radiator installations, whether belly- or freely exposed type, the aerodynamic efficiency of the core is comparatively unimportant and subordinate to the problem of proper radiator installation.

The heating effect on the minimum drag of radiators is noteworthy; although by the usual installation efficiency of belly radiators, at the present time the heating effect is only at about 10 percent lower drag than the unheated radiator (high-temperature liquid-cooling).

Translation by J. Vanier,
National Advisory Committee
for Aeronautics.

## REFERENCES


### Characteristics of Radiator Cores

1. Parsons and Haper: Radiators for Aircraft Engines. National Bureau of Standards Paper No. 211, May 1922 (fig. 19).

2. Lorenz, H.: Wärmeabgabe und Widerstand von Kühlerelementen. Abh. a.d. Aerod. Inst. an der Tech. Hochs. Aachen, Heft 13 (1935), S. 30.

### Drag and Flow through Ducted Radiators

3. Linke, W, and Friedrichs, W.: Untersuchungen über die Güte neuerer Kühlerelemente. (To be published in Luftfahrtforschung.)

4. Linke, W., and Friedrichs, W.: Der Einfluss der Öffnungsverhältnisse auf Widerstand und Durchfluss. (To be published in Luftfahrtforschung.)

5. Barth, W.: Die Bestimmung des Widerstands und der Durchflussmenge von Kühlern bei verschiedenen Einbauordnungen. Luftfahrtforschung, Bd. 14 (1937), S. 300.

### Effect of Heat on Radiator Drag

6. Meredith, F. W.: Note on the Cooling of Aircraft Engines with Special Reference to Ethylene Glycol Radiators Enclosed in Ducts. R. & M. No. 1683, British A.R.C., 1936.

7. Weise, A.: The Conversion of Energy in a Radiator. T.M. No. 869, N.A.C.A., 1938.

### General Reports on Heat Transfer and Friction Drag

8. Blasius; Das Ähnlichkeitsgesetz bei Reibungsvorgängen. Mitteilungen über Forschungsarbeiten des V.D.I., Heft 131 (1912), S. 12.

9. Merkel: Die Grundlagen der Warmeübertragung (1927).

10. Eisner: Reibungswiderstand, Hydromechanische Probleme des Schiffsantriebs (1932), S. 17.

11. Bosch, Maurits ten: Die warmeubertragung. J. Springer, Berlin, 1936.

General

12. Eick, H.: Mindestwiderstand von Schnellflugzeugen. Luftfahrtforschung, Lfg. 9, Bd. 15 (1938), S. 445.

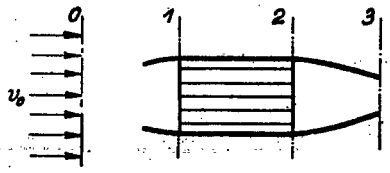


Figure 1.- Section notation for built-in radiator.

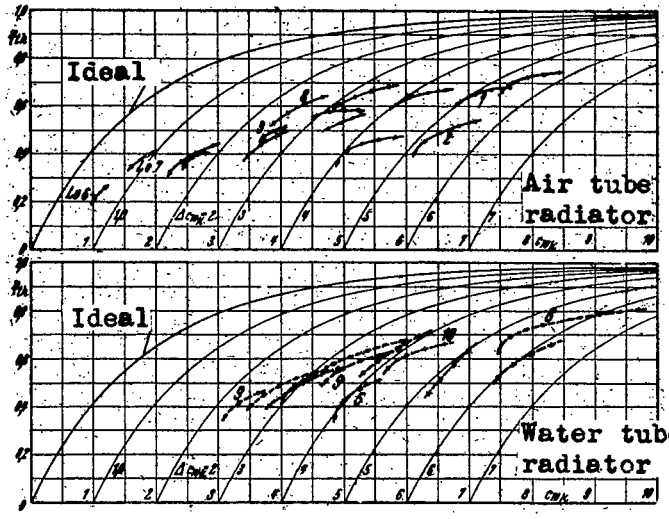


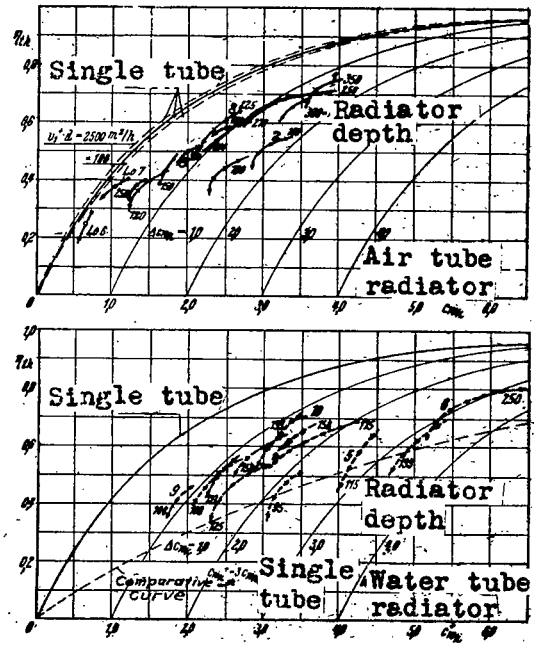


$c^+_{wk}$ referred to mean velocity $v^+_1$ in cooling passages.

Figure 3.- Pressure drop coefficient $c^+_{wk}$ of cold radiator and thermodynamic efficiency $\eta_{th}$ for different cooling systems (Table 1).

$c_{wk}$ referred to velocity $v_1$ directly before the core.

Figure 2.- Pressure drop coefficient $c_{wk}$ of cold radiator and thermodynamic efficiency $\eta_{th}$ for different cooling systems (Table 1).

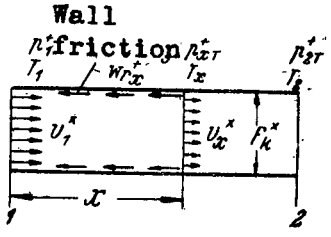


Figure 4.- Velocity, pressure and temperature notation in heated cooling tube.

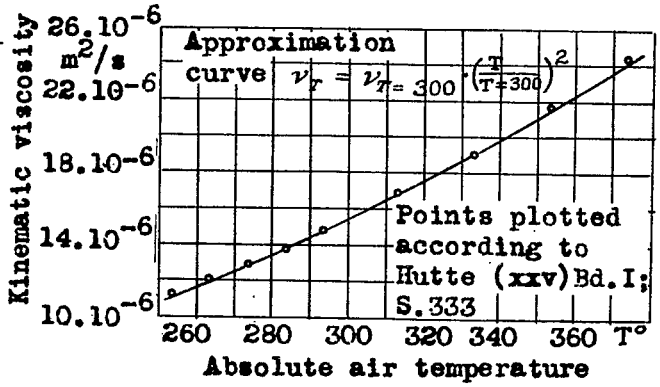


Figure 5.- Kinematic viscosity of air against temperature.

Table 1. Examined cooling systems.

| | No. | Identification | f = free section ratio | Test points |
|---|---|---|---|---|
| Air tube radiator | 1 | NKF Flat tube 8 x 2 | 0.69 | ○ |
| | 2 | NKF Jfa-gills | 0.69 | ▲ |
| | 3 | NKF- Hexagon tube 7/8 | 0.725 | × |
| | 8 | HW Special tube 9 x 3 | 0.76 | ◆ |
| | Lo6 Lo7 | Lorenz 6; 7 | 0.78 | □ |
| Water tube radiator | 5 | SKF-Behr- finned tube 226 | 0.80 | △ |
| | 6 | SKF-Behr- finned tube 240 | 0.83 | □ |
| | 9 | HW High performance radiator (h = 2.7) | 0.75 | ● |
| | 10 | HW- High performance radiator (h = 2.3) | 0.74 | ◇ |

| v | 16m/s | 28m/s |
|---|---|---|
| $c_{wk}$ | 7.33 | 6.87 |
| $\eta_{th}$ | .672 | .626 |

Figure 6.- NKF flat tube radiator 8×2×300 mm; free section ratio f = 0.69.

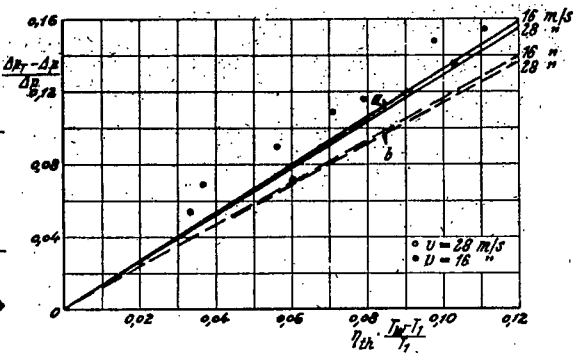


(a) Pressure difference between inlet and exit opening of core.

(b) Difference between pressures almost directly before and aft of the core.

Figure 7.- Computed rise in pressure drop due to heating of core compared to Aachen test values.

| v | 26.5m/s | 30.5m/s |
|---|---|---|
| $c_{wk}$ | 1.33 | 1.21 |
| $\eta_{th}$ | .175 | .172 |

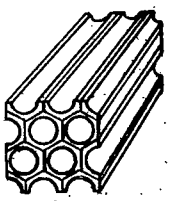

Figure 8.- Round tube radiator 6×35 mm diam. x 101.5 mm (Bureau of Standards); free section ratio f = 0.611.

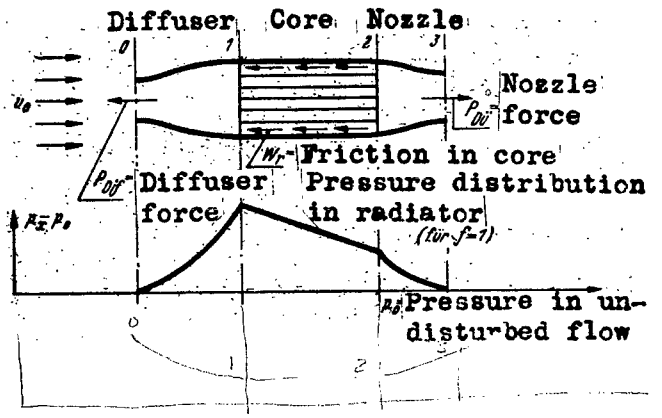


Figure 9.- Freely exposed radiator with pressure distribution.

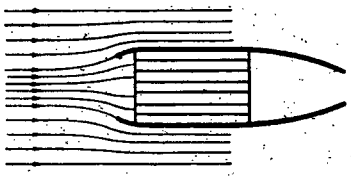

Figure 10.- Deflection of streamlines through the diffuser.

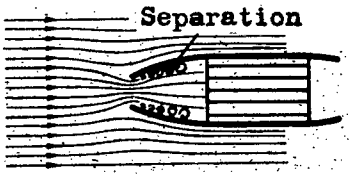


Figure 11.- Streamline pattern for two narrow diffusers.

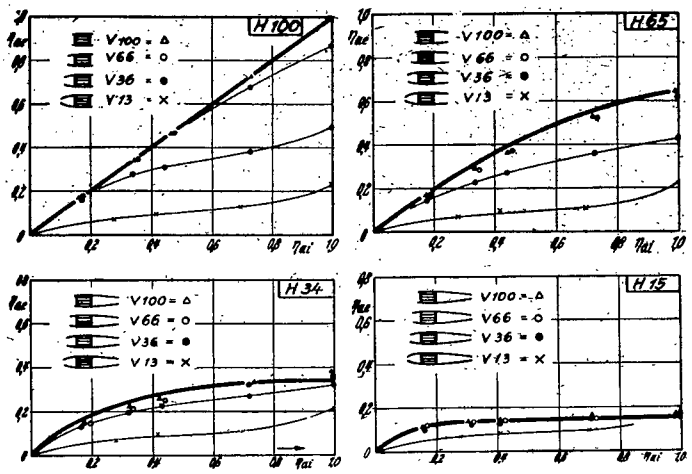


Comparison of computed (solid curve) and observed values at Aachen Δ o • ×. ($v_1$ = flow velocity through core, $v_0$ = velocity for upstream from radiator, $c_{wk}$ = pressure drop coefficient of unheated core).

Figure 12.- Flow coefficient $\eta_{ae} = v_1/v_0$ of freely exposed radiators against core permeability.

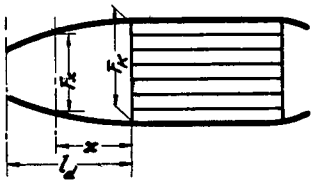


Figure 17.-Notation for interior surfaces of diffuser.

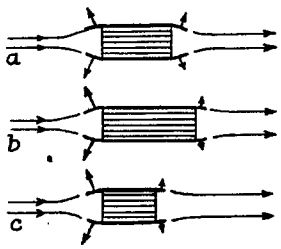


(a) Original radiator.
(b) reduced core permeability (unheated).
(c) increased kinetic energy of emerging airflow due to heating.
(d) equal pressure drop in core as assumed in (a).

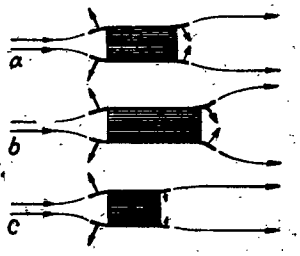


Sketch 1.- Diffuser and nozzle forces for case 1 for equal airflow.

$(F_3/F_2 < 1)$

Sketch 2.- Diffuser and nozzle forces for case 2 for equal airflow.

$(F_3/F_2 < 1)$

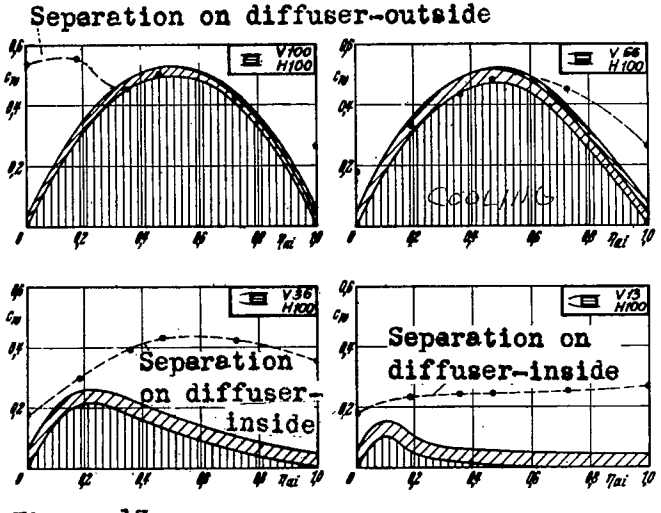


Figure 13.-

• = Aachen test data

▥ = internal cooling drag

▨ = skin friction drag

▩ = internal friction drag

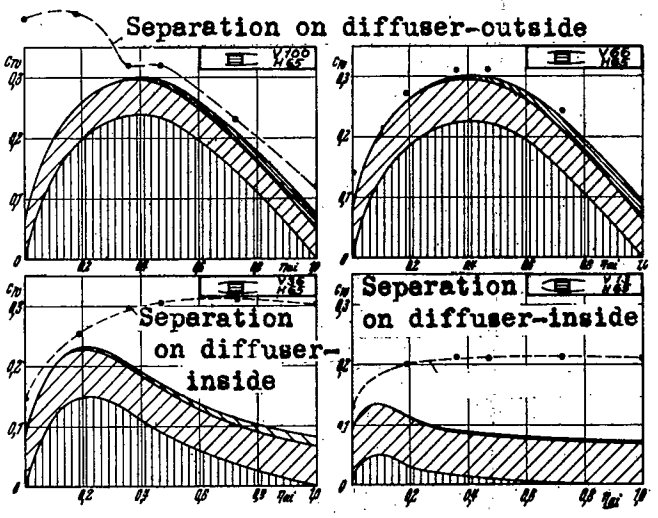


Figure 14.-

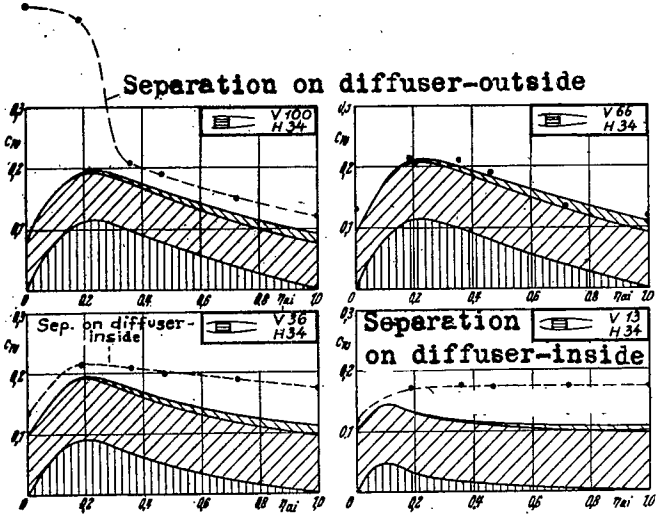


Figure 15.-

Figures 13-16.- Drag coefficients $c_w = W/\rho/2\ v_o^2\ F_k$ of unheated, freely exposed radiators in relation to core permeability $\eta_{ai} = \sqrt{1/1 + c_{wk}}$

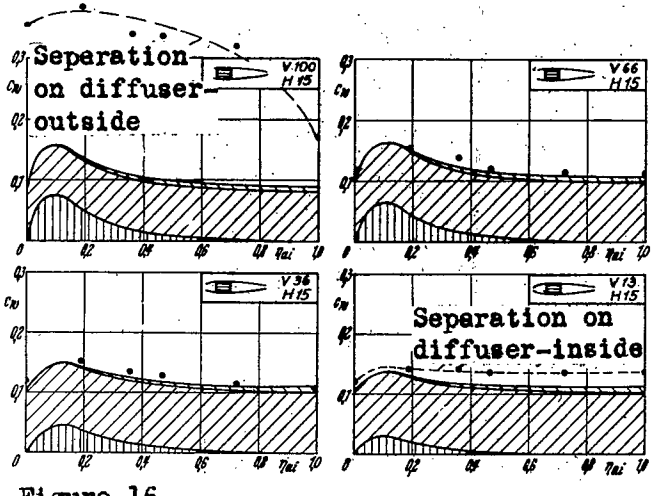


Figure 16.-

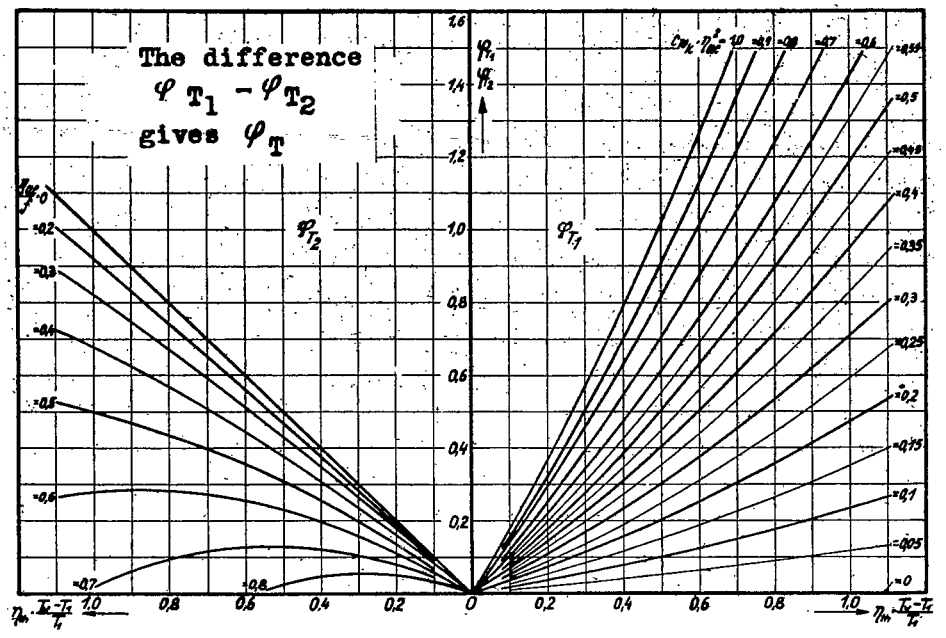


Figure 18a.- Chart defining influence quantity $\varphi_T$; large temperature range (hot and cold radiator adjusted to equal airflow $\eta_{ae}$).

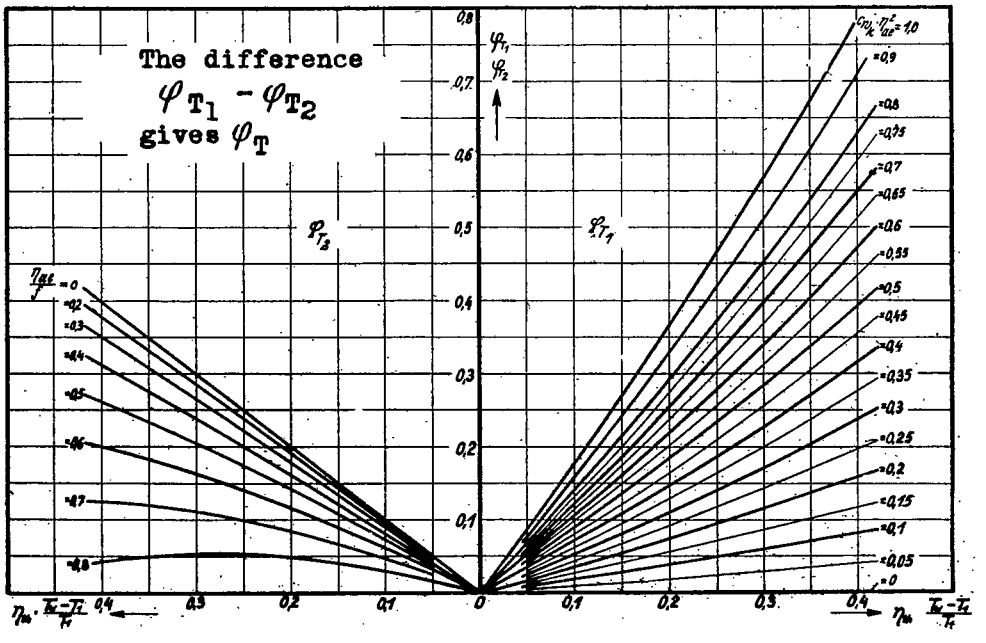


Figure 18b.- Chart defining influence quantity $\varphi_T$; small temperature range (hot and cold radiator adjusted to equal airflow $\eta_{ae}$).

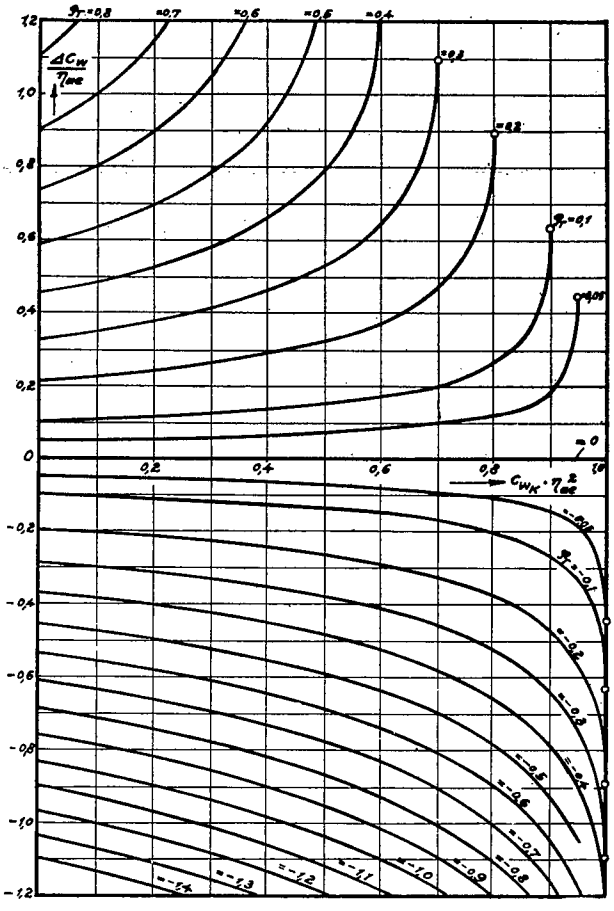

Figure 19.- Change in radiator drag $\Delta c_w$ due to heating for equal $\eta_{ae}$ in heated and unheated stage.

$\Delta c_w > 0$ = drag increase due to heating, $c_{wk}$ = drag coefficient of unheated core, $\eta_{ae} = v_1/v_0$ = flow coefficient.

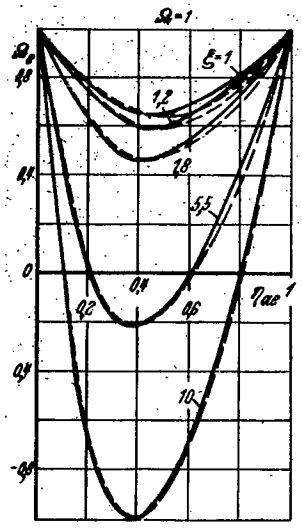

$$\xi = \frac{T_w}{T_1} = \frac{\text{Absolute wall temperature}}{\text{Absolute air inlet temperature}}$$

Figure 21.- Nondimensioned drag of radiators without nozzle (Weise, solid curve) compared with approximations of present report (dashed curve).

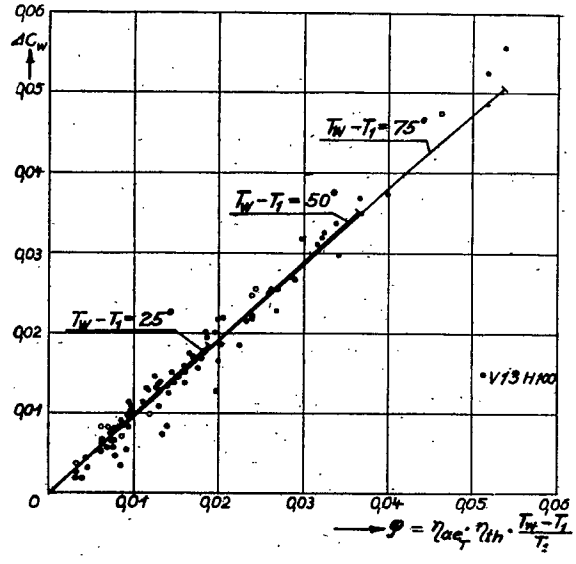

○ ● Aachen test data
—— Computed according to present report

Figure 20.- Change in radiator drag coefficients due to heating (diffuser and nozzle at same setting cold and heated).

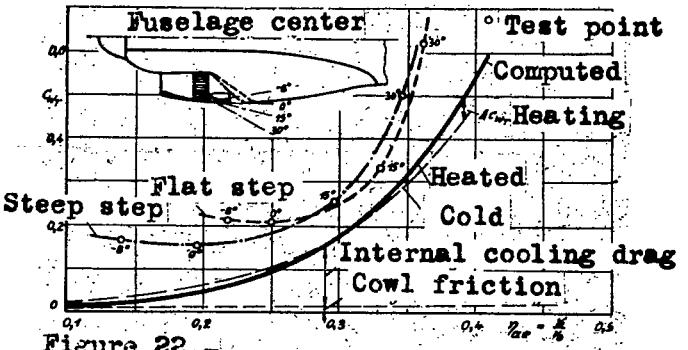


Figure 22.-

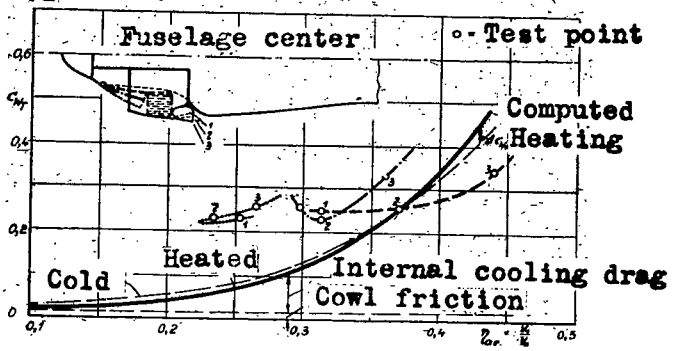


$c_{wT}$ = drag coefficients of heated radiator referred to frontal arc of radiator.

$\eta_{ae} = v_1/v_0$ = flow coefficient.

Figures 22 and 23.- Tests on belly radiators in the big DVL wind tunnel (Schlupp). Heated radiator into 57°C temperature difference between cooling agent and incoming air.

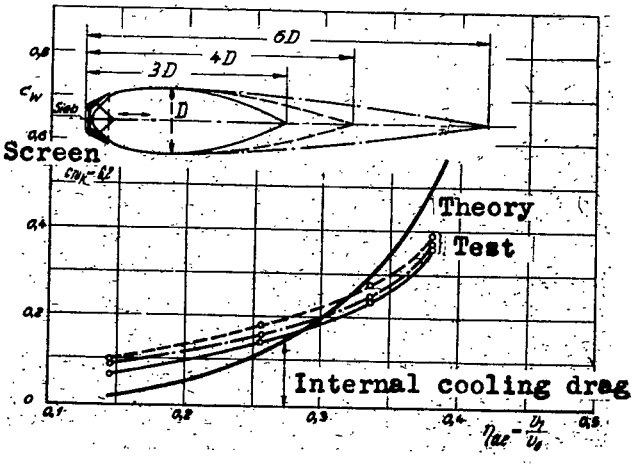


$c_w$ = drag coefficient of radiator referred to frontal area of radiator.

$\eta_{ae}$ = $v_1/v_0$ = flow coefficient.

Figure 24.- Tests on belly radiators in the small DVL tunnel, (Zobel). Cold radiator.